The Journal of Experimental Biology 204, 2943–2958 (2001)
Printed in Great Britain © The Company of Biologists Limited 2001
JEB3613

Locomotor function of the dorsal fin in teleost fishes: experimental analysis of wake forces in sunfish

Eliot G. Drucker[1,*] and George V. Lauder[2]

[1]*Department of Ecology and Evolutionary Biology, University of California, Irvine, CA 92697, USA* and
[2]*Museum of Comparative Zoology, Harvard University, 26 Oxford Street, Cambridge, MA 02138, USA*

*e-mail: edrucker@uci.edu

Accepted 12 June 2001

Summary

A key evolutionary transformation of the locomotor system of ray-finned fishes is the morphological elaboration of the dorsal fin. Within Teleostei, the dorsal fin primitively is a single midline structure supported by soft, flexible fin rays. In its derived condition, the fin is made up of two anatomically distinct portions: an anterior section supported by spines, and a posterior section that is soft-rayed. We have a very limited understanding of the functional significance of this evolutionary variation in dorsal fin design. To initiate empirical hydrodynamic study of dorsal fin function in teleost fishes, we analyzed the wake created by the soft dorsal fin of bluegill sunfish (*Lepomis macrochirus*) during both steady swimming and unsteady turning maneuvers. Digital particle image velocimetry was used to visualize wake structures and to calculate *in vivo* locomotor forces. Study of the vortices generated simultaneously by the soft dorsal and caudal fins during locomotion allowed experimental characterization of median-fin wake interactions.

During high-speed swimming (i.e. above the gait transition from pectoral- to median-fin locomotion), the soft dorsal fin undergoes regular oscillatory motion which, in comparison with analogous movement by the tail, is phase-advanced (by 30 % of the cycle period) and of lower sweep amplitude (by 1.0 cm). Undulations of the soft dorsal fin during steady swimming at 1.1 body length s^{-1} generate a reverse von Kármán vortex street wake that contributes 12 % of total thrust. During low-speed turns, the soft dorsal fin produces discrete pairs of counterrotating vortices with a central region of high-velocity jet flow. This vortex wake, generated in the latter stage of the turn and posterior to the center of mass of the body, counteracts torque generated earlier in the turn by the anteriorly positioned pectoral fins and thereby corrects the heading of the fish as it begins to translate forward away from the turning stimulus. One-third of the laterally directed fluid force measured during turning is developed by the soft dorsal fin. For steady swimming, we present empirical evidence that vortex structures generated by the soft dorsal fin upstream can constructively interact with those produced by the caudal fin downstream. Reinforcement of circulation around the tail through interception of the dorsal fin's vortices is proposed as a mechanism for augmenting wake energy and enhancing thrust.

Swimming in fishes involves the partitioning of locomotor force among several independent fin systems. Coordinated use of the pectoral fins, caudal fin and soft dorsal fin to increase wake momentum, as documented for *L. macrochirus*, highlights the ability of teleost fishes to employ multiple propulsors simultaneously for controlling complex swimming behaviors.

Key words: swimming, maneuvering, locomotion, dorsal fin, vortex wake, wake interaction, flow visualization, digital particle image velocimetry, bluegill sunfish, *Lepomis macrochirus*.

Introduction

Change in fin morphology and position is a central component of the evolutionary transformation of functional design in ray-finned fishes (Actinopterygii). Documenting phylogenetic patterns in the structure of the paired and median fins, and interpreting the functional significance of such patterns, has been the subject of ongoing study by systematists, functional morphologists and hydrodynamicists (e.g. Breder, 1926; Harris, 1953; Aleev, 1969; Lighthill, 1969; Gosline, 1971; Alexander, 1974; Rosen, 1982; Lauder, 2000). Of the propulsors employed by fishes, one of the least well understood from a mechanistic perspective is the dorsal fin, which is characterized by an evolutionary trend of anatomical elaboration. The plesiomorphic condition exhibited by most basal teleost fishes is the possession of a single soft-rayed dorsal fin (e.g. Fig. 1: Clupeiformes, Salmoniformes). In contrast, more derived teleosts typically have two distinct dorsal fins, the first (anterior) stiffened by spines and the second (posterior) soft-rayed (Lauder and Liem, 1983;

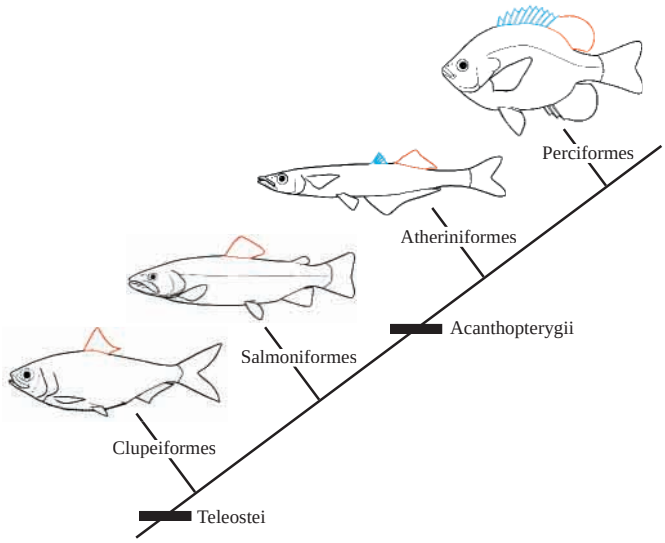

Fig. 1. Interrelationships among selected orders of teleost fishes to illustrate variation in dorsal fin design (see Lauder and Liem, 1983). Basal teleosts (e.g. Clupeiformes and Salmoniformes) typically possess a single, soft-rayed dorsal fin (shown in red). Most acanthopterygian fishes have, in addition, a spiny dorsal fin (shown in blue) positioned anterior to the soft-rayed portion. The two fins may be either contiguous (e.g. Perciformes) or separated by a gap (e.g. Atheriniformes). In this study, we investigate the wake generated by the soft dorsal fin of *Lepomis macrochirus*, a representative perciform fish, to explore the functional role of this conserved feature of teleostean locomotor anatomy. Fish images modified from Nelson (Nelson, 1994).

Helfman et al., 1997). This apomorphic condition characterizes most acanthopterygian fishes, including species with a distinct separation between the spiny and soft dorsal fins as well as species in which these fin sections are fused (Fig. 1; cf. Atheriniformes, Perciformes). In spite of this significant anatomical variation, we have only a very limited understanding of the hydrodynamic significance of evolutionary transformations in dorsal fin design within teleost fishes.

Studies of locomotor anatomy and behavior have identified a number of specialized swimming modes involving activity of the dorsal fin (summarized by Breder, 1926; Lindsey, 1978; Braun and Reif, 1985; Webb, 1993). Fishes may swim steadily by undulating the soft dorsal fin alone, as in the bowfin *Amia calva* (Breder, 1926), or by undulating or flapping the dorsal fin in concert with other fin surfaces, as in tetraodontiform fishes (Harris, 1937; Blake, 1977; Blake, 1978; Lighthill and Blake, 1990; Arreola and Westneat, 1996; Gordon et al., 2000), seahorses (Breder and Edgerton, 1942; Blake, 1976) and the crossopterygian fish *Latimeria chalumnae* (Fricke and Hissmann, 1992). In unsteady swimming (i.e. fast-start acceleration and turning), the potential hydromechanical role played by the dorsal fin has also been explored through kinematic analysis (Blake, 1976; Blake, 1977; Jayne et al., 1996), mathematical modeling (Weihs, 1972a; Weihs, 1973), fin amputation (Harris, 1936; Webb, 1977) and computational fluid dynamics (Wolfgang et al., 1999). Although encompassing a broad taxonomic range of fishes, existing biomechanical studies of the teleost dorsal fin have largely excluded consideration of the Perciformes, the largest and most diverse order of bony fishes with approximately 9300 species (Helfman et al., 1997).

In this paper, we initiate empirical hydrodynamic study of the locomotor functions served by the perciform dorsal fin through the use of quantitative wake visualization. The bluegill sunfish (*Lepomis macrochirus*) is selected as a representative perciform fish, exhibiting the characteristic dual dorsal-fin anatomy (Fig. 1), for which patterns of fin movement and motor activity during swimming are well described (Jayne et al., 1996). Our experimental analysis focuses on the soft-rayed dorsal fin, the plesiomorphic portion of the dorsal fin that has been retained throughout teleost evolution. We address two specific questions regarding the function of the soft dorsal fin in sunfish. First, what locomotor role, if any, is played by the fin during steady swimming and unsteady turning maneuvers? Functions traditionally ascribed to the dorsal fin of perch-like fishes have been largely non-propulsive. During steady swimming, for instance, the fin has been described as hydrodynamically inactive when furled (Webb and Keyes, 1981) or as a keel or body stabilizer when erected (Aleev, 1969). During turning, the dorsal fin has been proposed to serve as a pivot point, again playing a largely passive, non-propulsive role (Helfman et al., 1997). In this paper, we study the wake shed by freely swimming fish to determine experimentally the extent to which propulsive force is generated by the dorsal fin. Second, do wake structures shed by the soft dorsal fin either positively or negatively influence the wake and associated fluid forces of the tail downstream? This question is addressed in the light of previous theoretical work emphasizing the potential for wake interaction among nearby fish fins to increase propulsive efficiency (Lighthill, 1970; Wu, 1971b; Yates, 1983; Weihs, 1989).

Our overall goal is to begin an experimental hydrodynamic analysis of dorsal fin function through study of the soft dorsal fin in sunfish. The aim of future work will be to examine the locomotor roles of the spiny dorsal fin in derived teleosts as well as the soft dorsal fin in more basal clades. Investigating dorsal fin function by means of quantitative flow visualization contributes to a growing body of literature on the experimental hydrodynamics of animal swimming and is intended to clarify the biomechanical role of a key anatomical feature of teleost fishes.

Materials and methods

Fish

Bluegill sunfish (*Lepomis macrochirus* Rafinesque) were collected by seine from ponds in Newport Beach, CA, USA. Study of median fin function in *L. macrochirus* allowed direct comparisons with previous work with this species on wake flow dynamics during pectoral fin locomotion (Drucker and Lauder, 1999; Drucker and Lauder, 2000; Drucker and Lauder,

2001). Animals were maintained at 20 °C in 40 l freshwater aquaria and fed earthworms twice weekly. Four fish of similar size (total body length, L, 21.0±1.2 cm, mean ± S.D.) were selected for wake visualization experiments.

Swimming protocol and wake visualization

Sunfish swam individually in the center of the working area (28 cm×28 cm×80 cm) of a variable-speed freshwater flow tank. Steady swimming was elicited at two speeds: $0.5\,L\,s^{-1}$ (approximately $11\,cm\,s^{-1}$), a speed at which propulsion was achieved by oscillation of the paired pectoral fins without contribution from the median fins, and $1.1\,L\,s^{-1}$ (approximately $23\,cm\,s^{-1}$), a speed just above the gait transition to combined paired- and median-fin locomotion (for animals of the size studied here, this gait transition speed is $1.0\,L\,s^{-1}$; Drucker and Lauder, 2000). In addition, sunfish performed unsteady turns in response to a visual and auditory stimulus. While fish swam steadily at $0.5\,L\,s^{-1}$, a wooden dowel was introduced into the water along the wall of the working area inducing a low-speed evasive maneuver, as described previously (Drucker and Lauder, 2001).

During both steady swimming and unsteady turning behavior, the wake shed by the soft dorsal fin was studied experimentally using digital particle image velocimetry (DPIV) (for details of the method, see Willert and Gharib, 1991; Drucker and Lauder, 1999; Lauder, 2000). The flow-visualization system employed in this study was a slight modification of that described by the authors in earlier work (Drucker and Lauder, 2001). A 5 W argon-ion laser was focused into a sheet of light 16 cm wide and used to illuminate reflective microspheres suspended in the flow. In separate DPIV experiments, it is possible to reorient the light sheet into three perpendicular orientations, allowing three-dimensional reconstruction of wake geometry (Drucker and Lauder, 1999). In the present study, the dorsal fin wake was visualized in the horizontal (frontal) plane and videotaped from a dorsal perspective by means of a mirror inclined at 45 ° above the working area. Vertically oriented laser sheets (i.e. in the parasagittal and transverse planes) projected from below were obstructed by the body of the fish itself and were therefore not employed. However, previous DPIV work examining flow within orthogonally oriented laser planes supports a three-dimensional vortex-ring wake structure for the median fins of fishes (Wolfgang et al., 1999; Lauder, 2000; Liao and Lauder, 2000). On this basis, we used flow measurements from frontal-plane transections of the dorsal fin wake to estimate vortex ring morphology and associated fluid forces generated during locomotion.

A dual-camera high-speed video system (NAC HSV-500c^3) was used to record simultaneous images of both the fish and its wake at 250 frames s^{-1} (1/500 s shutter speed). Lateral video images (Fig. 2A,B) provided a reference view of the trailing edge of the dorsal fin and the vertical position of the horizontal laser plane. Synchronized dorsal-view video images (Fig. 2C) revealed patterns of particle movement within the frontal plane in real time. The horizontal light sheet was positioned at three heights along the dorsoventral body axis of the fish. In its highest position (Fig. 2D, position 1), the laser plane intersected the middle of the soft dorsal fin, allowing measurement of the structure and strength of shed vortices and estimation of the momentum added to the dorsal fin wake during both steady swimming and turning. In its intermediate position (Fig. 2D, position 2), the laser plane intersected both the ventral portion of the soft dorsal fin and the dorsal lobe of the tail. This configuration enabled direct observation of the interaction between the wakes shed by the two adjacent fins. In its lowest position (Fig. 2D, position 3), the laser plane intersected the tail at mid-fork. Flow patterns within this plane were used to characterize the structure of the tail's wake and to estimate caudal-fin swimming forces, which provided a context for interpreting calculated dorsal fin forces.

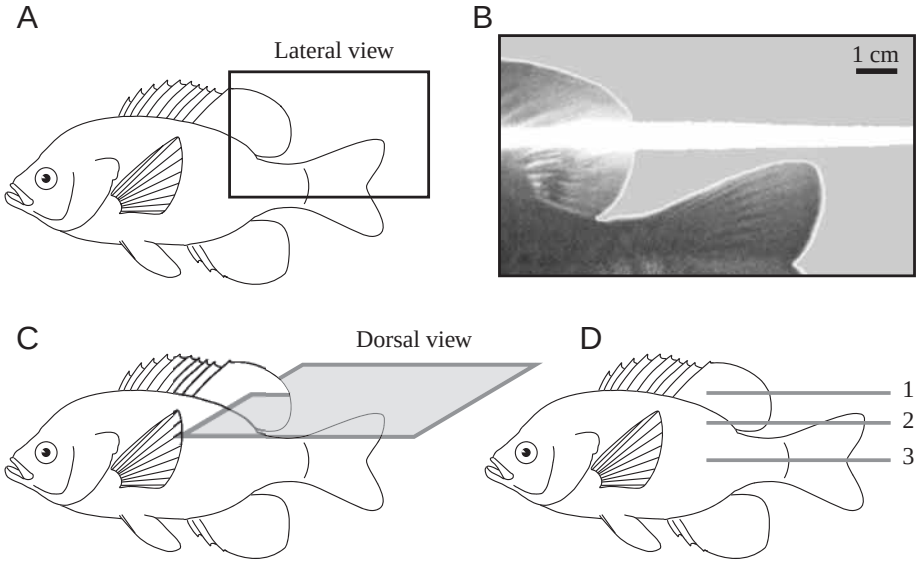

Fig. 2. Experimental approach for visualizing the median fin wake. (A) Within the region bound by the rectangle, lateral video images of bluegill sunfish were recorded during steady swimming at both low and high speed and during unsteady turning maneuvers. (B) Representative lateral-view reference image showing the dorsal lobe of the tail and the trailing edge of the soft dorsal fin intercepted by a horizontal (frontal-plane) laser sheet seen on edge as a white stripe. (C) Synchronized dorsal-view video of this laser sheet allowed analysis of wake flow using digital particle image velocimetry (see Materials and methods). (D) To study the wake structures and fluid forces generated by the soft dorsal and caudal fins, flow was analyzed within laser planes at three heights (1–3). Fin movements and the resulting fluid flow within these planes are illustrated in Figs 3–8 and Fig. 10.

Kinematic and hydrodynamic measurements

From DPIV video tapes, 68 swimming events performed by four fish were reviewed to establish general patterns of propulsor motion and water flow in the wake. Of these events, 12 each were selected for detailed analysis of dorsal fin activity during steady swimming and unsteady turning. Kinematic and hydrodynamic measurements were also made from 16 cycles of caudal-fin oscillation. In addition, 25 video sequences of fluid flow within laser planes intersecting both the dorsal and caudal fins simultaneously (Fig. 2D, position 2) were inspected to study median-fin wake interaction.

For the purpose of calculating stroke-averaged locomotor force, the duration of propulsive fin movement τ was measured from each swimming sequence. For steady swimming, τ was defined as the stroke period of median fin oscillation (i.e. the interval in milliseconds separating the position of maximal left or right excursion of the fin tip and the analogous position in the immediately following stride). For turning, during which vortical wake structures were generated over the course of a single half-stroke, τ was taken as the duration of dorsal fin abduction and following adduction to the midline. To characterize temporal and spatial patterns of median fin movement during steady swimming, selected video frames were digitized using custom-designed image-analysis software. In every other frame (i.e. at 8 ms intervals), the trailing edges of the soft dorsal fin and caudal fin within the horizontal light sheet were assigned *x*,*y* Cartesian coordinates. Each fin beat cycle was thus represented by approximately 50 digitized points. These data allowed graphical presentation of two-dimensional fin tip trajectories as well as measurement of the relative sweep amplitude and phase lag of oscillatory motion of the dorsal and caudal fins. The Strouhal number (*St*) was calculated for each fin during steady swimming as a predictor of vortex wake structure and propulsive efficiency (Triantafyllou et al., 1993; Anderson et al., 1998):

$$St = fA/U, \quad (1)$$

where f is fin beat frequency, A is wake width (estimated as maximal side-to-side excursion of the fin's trailing edge) and U is the forward swimming speed of the fish.

Two-dimensional water velocity fields in the wake of sunfish were calculated from consecutive digital images (640×480 pixels) by means of spatial cross-correlation (Willert and Gharib, 1991; Raffel et al., 1998). In total, 171 image pairs from steady swimming and turning events by the four experimental animals were processed for calculation of wake structure and strength (for details, see Drucker and Lauder, 1999). Frontal-plane flow fields were typically 7–10 cm on each side and made up of 20×20 matrices of velocity vectors. Vectors overlying the body or fins, or falling within regions of shadow cast by the fish, were misrepresentative of actual water flow and deleted manually from flow fields. From each vector matrix, the mean velocity and orientation of the fluid jet between paired counterrotating vortices were measured. Jet velocity was taken as the average magnitude of vectors comprising the central region of accelerated flow within the frontal plane after mean free-stream flow velocity had been subtracted. For both steady swimming and turning behavior, jet angle was defined as the average orientation of velocity vectors comprising the fluid jet, measured relative to the heading of the fish at the onset of the fin stroke (see also Drucker and Lauder, 2001).

In the absence of information about wake flow in three dimensions, fluid forces produced during locomotion were estimated from frontal-plane velocity fields. We assumed that paired vortices observed in the frontal plane represent approximately mid-line sections of a circular vortex ring. The momentum of the ring was calculated as the product of water density, mean vortex circulation and ring area (πR^2, where R is half the distance between paired vortex centers). Stroke-averaged wake force was then computed as the reaction to the rate of change in wake momentum (i.e. the fluid momentum added to the wake by the fins over the stroke duration τ; see Milne-Thomson, 1966). Further details of the calculation of wake force by this method can be found in earlier studies (Spedding et al., 1984; Dickinson, 1996; Dickinson and Götz, 1996; Drucker and Lauder, 1999). The total force exerted by each median fin was resolved geometrically into perpendicular components within the frontal plane (thrust and lateral force) according to the mean jet angle. For both steady swimming and turning, force components were measured relative to the axis of progression of the fish at the onset of fin abduction (see also Drucker and Lauder, 2001).

Results

Dorsal fin wake: flow patterns and locomotor forces

During steady locomotion, the wake of the dorsal fin of sunfish shows pronounced structural variation with swimming speed. At the lower swimming speed studied ($0.5\,L\,s^{-1}$), all the median fins are hydrodynamically inactive as the paired pectoral fins alone propel the animal forward. The spiny and soft dorsal fins remain parallel to the fish's heading and cause no large-scale deflection of the incident flow. In regions immediately upstream and lateral to the dorsal fin (Fig. 3A), as well as in the near-field wake posterior to the fin (Fig. 3B), water flow remains in an undisturbed downstream-oriented direction. In contrast, during higher-speed swimming at $1.1\,L\,s^{-1}$, the median fins are recruited to supplement swimming forces generated by the oscillating pectoral fins. At speeds above the gait transition from purely pectoral-fin locomotion to combined pectoral- and median-fin propulsion, the undulating soft dorsal fin sheds a well-defined vortex wake (Fig. 4). Although the trailing edge of the dorsal fin shows generally similar kinematics to that of the tail, the upstream and downstream median fins create distinct and independent momentum flows.

Each half-stroke of the soft dorsal fin involves excursion from a maximally abducted position to a corresponding contralateral position. As the fully abducted dorsal fin begins to sweep inwards towards the midline of the body, flow converges on the concave surface of the fin (Fig. 4A). On the

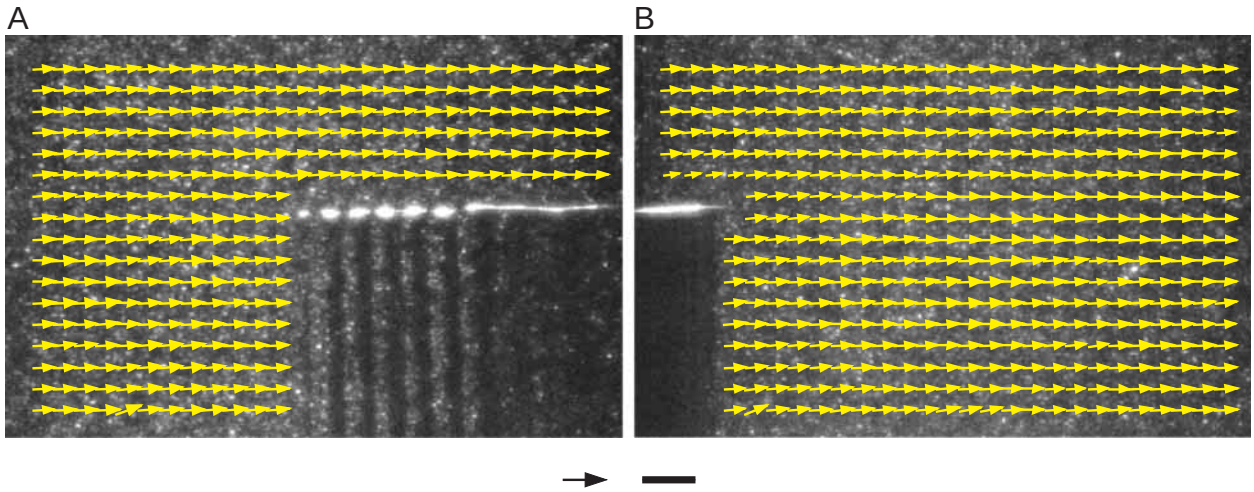

Fig. 3. Frontal-plane water velocity vector fields in the vicinity of the dorsal fin during swimming by sunfish at $0.5\,L\,s^{-1}$ ($10.5\,cm\,s^{-1}$), where L is total body length. (A) Laser plane slightly above position 1 (see Fig. 2D) to illuminate the leading edge of the spiny dorsal fin (several fin spines are visible, each of which casts a discrete shadow) and the anterior portion of the soft dorsal fin (at right). (B) Laser plane at position 1 intersecting the trailing edge of the soft dorsal fin. At this low swimming speed, propulsion is achieved solely by oscillation of the paired pectoral fins (anterior to the field of view); the dorsal fin is not observed to oscillate. At a gross level, incident flow encountering the spiny dorsal fin (A) remains unchanged in orientation and velocity when measured downstream of the soft dorsal fin (B). Scales: arrow, $20\,cm\,s^{-1}$; bar, 1 cm.

next half-stroke, rotational flow can be seen projected away from the convex surface of the fin (Fig. 4C). This medial and lateral water flow, arising from regions of alternating low and high pressure on each side of the dorsal fin, helps develop and concentrate vorticity for shedding into the wake. In Fig. 4A, a counterclockwise-rotating 'starting vortex' (*sensu* Brodsky, 1991; Grodnitsky and Morozov, 1992; Grodnitsky and Morozov, 1993) is visible at the trailing edge of the soft dorsal fin (vortex I in Fig. 4E). Over the course of the stroke, this structure is shed as a free vortex (visible in the upper right-hand corner of Fig. 4B,C) and travels downstream to enter the wake. Opposite-sign vorticity bound to the dorsal fin upstream in the region of suction flow (see upper left-hand corner of Fig. 4A and vortex II in Fig. 4E) migrates posteriorly, forming a discrete 'stopping vortex' at the end of the half-stroke (see clockwise flow at the trailing edge of the fin in Fig. 4B and vortex II in Fig. 4F). The onset of the return stroke (Fig. 4C) results in a new starting vortex III (analogous to vortex I). During the stroke reversal, vortex III coalesces with the previous half-stroke's stopping vortex II to form a combined vortex II+III (Fig. 4G). As the fin decelerates at the end of its contralateral abduction (Fig. 4D), this combined vortex is visible in the wake downstream. A stopping vortex for the return stroke (IV) develops but remains attached to the fin tip at the end of the kinematic stroke period (Fig. 4H). (Note that, on the subsequent half-stroke, vortex IV fuses with a newly created vortex I to form a combined structure analogous to vortex II+III.) Thus, each complete beat of the soft dorsal fin generates a pair of free counterrotating vortices (I and II+III) within the horizontal wake plane. Continuously repeated cycles of fin oscillation result in an array of staggered vortices with downstream-directed fluid jets alternating on the left and right sides of the body. Velocity vectors within these momentum jets have a mean magnitude of $7\,cm\,s^{-1}$ above the free-stream flow velocity and an average orientation of 62 ° offset from the axis of progression of the fish (Table 1).

Low-speed (i.e. non-fast-start) turning maneuvers in sunfish are characterized by two kinematic stages: rotational and translational. In the initial stage of a turn, sunfish use unilateral pectoral fin abduction to generate a laterally oriented wake flow on the same side of the body as the given stimulus (Fig. 5A). A medially oriented reaction force, transmitted to the body through the pectoral fin base, causes yawing rotation of the animal at velocities up to $32\,°\,s^{-1}$. During the rotational phase of the turn (Fig. 5A,B), the center of mass of the body undergoes minimal side-slip. Upon completion of body rotation, both pectoral fins rapidly adduct; the fin contralateral to the stimulus generates a posteriorly directed momentum flow whose reaction helps propel the animal forward and away from the stimulus (Fig. 5B). In addition to these previously documented pectoral fin movements (Drucker and Lauder, 2001), the soft dorsal fin was also observed to become active during turning. After the rotational phase of the turn, and after the onset of pectoral fin adduction that marks the beginning of the translational phase, the trailing edge of the dorsal fin consistently abducts (Fig. 5B,C). A starting vortex is shed as the fin moves laterally (Fig. 5D,F, vortex I) and a counterrotating 'stopping-starting' vortex (Brodsky, 1991; Brodsky, 1994; Drucker and Lauder, 1999) is shed as the fin decelerates, completes its stroke reversal and returns to the midline of the body (Fig. 5E,G, vortex II+III). As during steady swimming at speeds above the gait transition, turning in sunfish involves the generation of paired vortices with a central fluid jet during the course of each fin stroke. Unlike

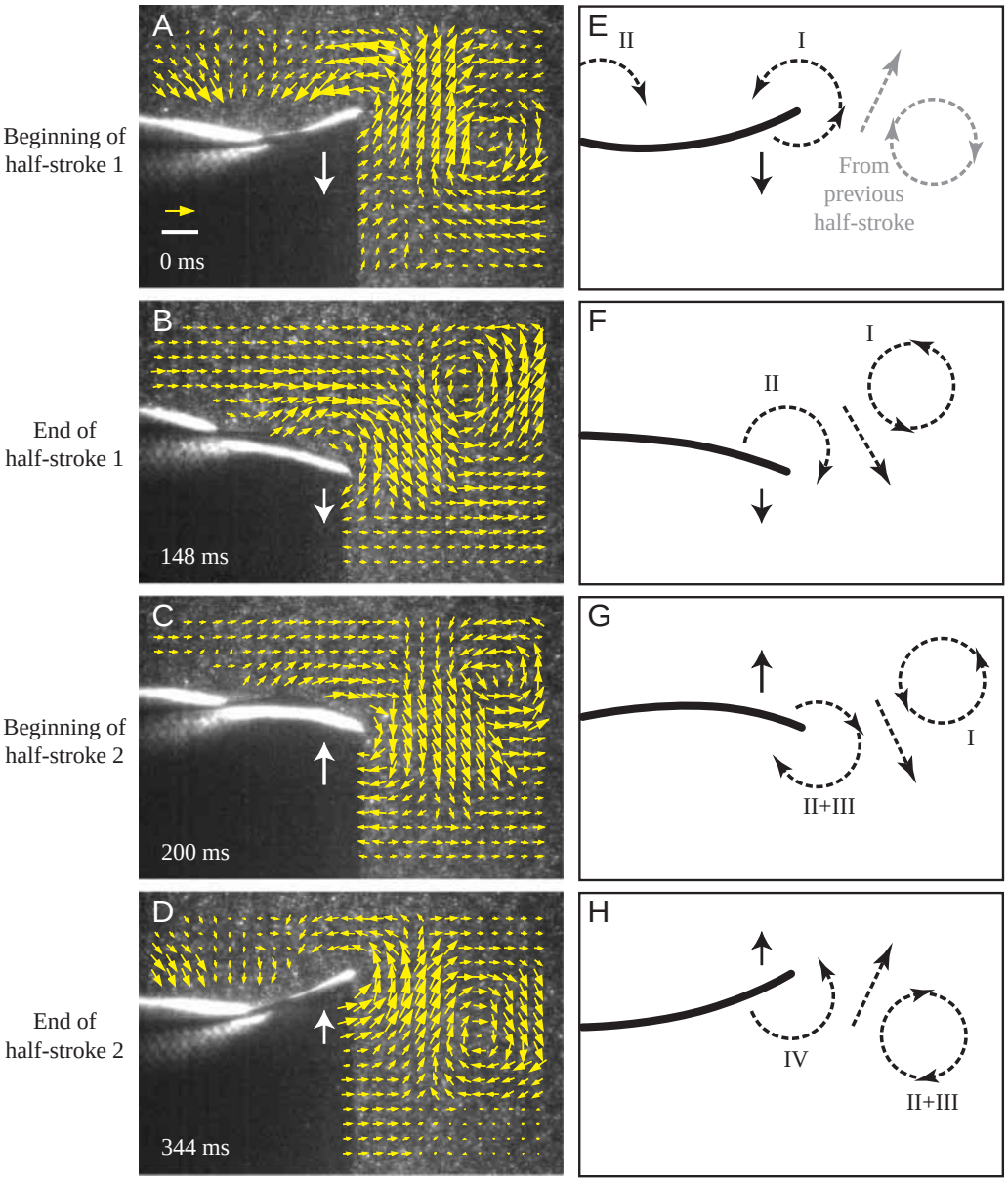

Fig. 4. Representative flow fields in the wake of the oscillating soft dorsal fin of sunfish during steady swimming at $1.1\,L\,s^{-1}$, where L is total body length. A–D show wake flow patterns within the frontal-plane laser sheet intersecting the middle of the soft dorsal fin (Fig. 2D, position 1) for two consecutive fin half-strokes. The direction of fin motion is indicated by large solid-line arrows. Free-stream velocity ($23.1\,cm\,s^{-1}$) from left to right has been subtracted from each velocity vector to reveal vortical wake structures. Schematic illustrations of these structures are given in E–H (observed vortices and fluid jets are represented by dashed-line arrows). At this relatively high swimming speed, the soft dorsal fin's activity causes substantial deflection and acceleration of the incident flow (cf. Fig. 3). (A) As the fin sweeps medially (here at the beginning of a half-stroke), a strong center of vorticity is generated at the fin's trailing edge, while opposite-sign vorticity bound to the fin develops upstream. These two rotational flows can be seen converging on the concave surface of the dorsal fin. Note that the jet and clockwise vortex at the right side of this panel were developed during the previous half-stroke in the opposite direction. (B) At the end of the half-stroke, vorticity is released from the trailing edge of the fin and shed into the wake as a free vortex (see counterclockwise flow). Vorticity previously attached to the anterior portion of the fin migrates downstream to contribute to new trailing edge vorticity (clockwise flow). (C) On the return half-stroke, trailing edge vorticity is strengthened and contributes to developing jet flow. (D) By the end of the return stroke, a second vortex has been shed into the wake (see clockwise flow), while opposite-sign, bound vorticity develops at the fin's trailing edge. Each complete fin stroke therefore creates a pair of free counterrotating vortices (I and II+III) with a central region of jet flow. Over repeated cycles of soft dorsal fin oscillation, a staggered trail of linked vortices is formed, with downstream jets alternating on the left and right sides of the body. From the momentum of this reverse von Kármán vortex street, stroke-averaged wake forces for propulsion can be calculated. Note that the vortices labeled I–IV in E–H are directly comparable with those illustrated for turning (see Fig. 5F,G). I, starting vortex of half-stroke 1; II, stopping vortex of half-stroke 1; II+III, stopping vortex of half-stroke 1 combined with same-sign starting vortex of half-stroke 2; IV, stopping vortex of half-stroke 2. Scales for A–D: arrow, $10\,cm\,s^{-1}$; bar, 1 cm.

steady swimming, however, turning is characterized by non-periodic dorsal fin motions and unilaterally applied fluid forces.

To define the role of the soft dorsal fin in controlling the turning maneuver, wake forces were resolved geometrically into perpendicular components within the frontal wake plane. These force components were measured relative to the rotated heading of the fish at the onset of dorsal fin abduction. In this study, we recorded DPIV video with a relatively high-magnification field of view that included the laser-illuminated flow field but that excluded much of the body of the fish (e.g. Fig. 3, Fig. 4, Fig. 5D,E). As a result, direct measurement of the orientation of the longitudinal body axis was rarely possible. However, in separate light-video recordings of turning (250 frames s^{-1}), we observed that body rotation is completed by sunfish well before the soft dorsal fin begins to abduct (temporal difference 43±7 ms, mean ± S.E.M., N=10). Therefore, average total body rotation (25.7 ° in yaw) was used to estimate the heading of the fish at the onset of dorsal fin movement. In Table 1, jet angles and fluid force components for turning are measured in relation to this initial heading axis. During turning, the wake jet of the dorsal fin has an average velocity that is similar to that during steady swimming at 1.1 L s^{-1} (7–8 cm s^{-1}). However, one-way analyses of variance reveal that the orientation of the jet and the magnitude of wake force differ significantly between the two behaviors (P<0.001). Steady swimming is characterized by dorsal-fin wake jets oriented 20 ° further laterally than those produced by turning (Table 1). In addition, the laterally and posteriorly directed components of force generated during unsteady turning maneuvers exceed those developed during steady swimming by 1.3- and 2.9-fold, respectively, on average (Table 1).

Table 1. *Kinematic and hydrodynamic measurements from dorsal- and caudal-fin swimming behaviors by bluegill sunfish*

	Dorsal fin		Caudal fin
Measurement	Steady swimming	Turning	Steady swimming
Duration of propulsive fin movement (ms)	404±8.5	261±16.1	398±9.8
Mean jet angle (degrees)	62.4±1.8	42.6±5.7	58.4±1.9
Mean jet velocity (cm s^{-1})	7.3±0.5	7.6±1.1	7.3±0.4
Force, lateral component (mN)	8.7±0.9	11.2±2.0	23.2±1.3
Force, posterior component (mN)	4.5±0.7	13.2±2.6	14.2±0.9
Force ratio, lateral:posterior	2.06±0.19	1.05±0.21	1.68±0.12
Strouhal number	0.19±0.01	–	0.31±0.01

Dorsal fin measurements are reported for steady swimming at 1.1 L s^{-1} and for turning immediately following steady swimming at 0.5 L s^{-1}. Caudal fin data are for steady swimming at 1.1 L s^{-1}. Mean body length L=21.0 cm.

All measurements are tabulated as mean ± S.E.M. (N=8–16 fin beats per behavior performed by four individuals for rows 1–6; N=25 for Strouhal number). Wake measurements are defined in the text and were made from frontal-plane velocity fields (see Fig. 2D; laser plane positions 1 and 3 were used for the dorsal and caudal fins, respectively). Note that jet velocities are measures taken above the mean free-stream flow velocity. Calculated lateral and posterior (thrust) forces are averages over the stroke duration (i.e. associated with a single vortex pair).

One-way analyses of variance were used to assess the significance of differences among the three behaviors (Bonferroni-adjusted significance level α=0.008). All dorsal fin measurements for steady swimming differed significantly from those for turning (P<0.001), except mean jet velocity and lateral wake force. During steady swimming, the dorsal and caudal fin wakes showed highly significant differences in the magnitude of laterally and posteriorly directed force (P<0.0001).

Median-fin wake interaction: kinematic and hydrodynamic measurements

To investigate potential hydrodynamic interactions between the dorsal and caudal fins, we measured median fin kinematics and corresponding wake flow patterns within the frontal plane (Fig. 2D, position 2). Above the gait transition speed, sunfish initiate axial undulation and exhibit sinusoidal motions of the dorsal fin and tail (Fig. 6A–D). The period of oscillation is not significantly different between the two fins (Table 1); median-fin beat frequency at 1.1 L s^{-1} is approximately 2.5 Hz. Temporal and spatial patterns of fin motion within the horizontal plane of analysis are presented for two consecutive stroke cycles in Fig. 6E. The trailing edges of the two fins move with an average phase lag of 121.4±2.0 ms (mean ± S.E.M., N=25 fin beat cycles), with the soft dorsal fin leading the dorsal lobe of the tail. The sweep amplitude (i.e. maximal side-to-side excursion) of the tail (2.69±0.08 cm, mean ± S.E.M.) significantly exceeds that of the dorsal fin (1.66±0.04 cm, mean ± S.E.M.) (unpaired t-test, d.f.=48; P<0.0001).

In the immediate vicinity of the dorsal and caudal fins, quantification of vortex flow was hindered by optical contamination of DPIV video. Shadows cast by the median fins obscured particles in a substantial portion of each video field (see Fig. 6A–D), thereby limiting the area available for cross-correlation. Flow fields calculated for regions including both fins were dominated by erroneous vectors representing propulsor motion rather than fluid flow. As a result, vortices in the region of the caudal peduncle (i.e. between the soft dorsal fin and tail) were studied closely in the raw video recording to allow vortex positioning relative to the paths taken by the median fins (Fig. 7). Since vortices shed by the dorsal fin develop as the propulsor begins to move medially from a position of maximal left or right abduction (Fig. 4), these wake structures are positioned in Fig. 7 precisely at the crests and troughs of the dorsal fin's sinusoidal trajectory. The path followed by the trailing edge of the tail consistently passes between the paired vortices shed by the dorsal fin. Specifically, because the caudal fin has a larger sweep amplitude than the dorsal fin (by an average of 0.51 cm on each side of the body), at the extremes of its left–right motion the former is positioned to intercept the wake of the latter

(Fig. 7). The tail itself generates a vortex wake very similar to that produced by the soft dorsal fin: a trail of staggered, counterrotating vortices arranged in pairs, each with a central fluid jet (Fig. 8). Although the average orientation and velocity of these jets are similar for the dorsal and caudal fins during steady swimming, the tail generates significantly greater laterally and posteriorly directed components of force (Table 1). The nature of the dorsal–caudal fin wake

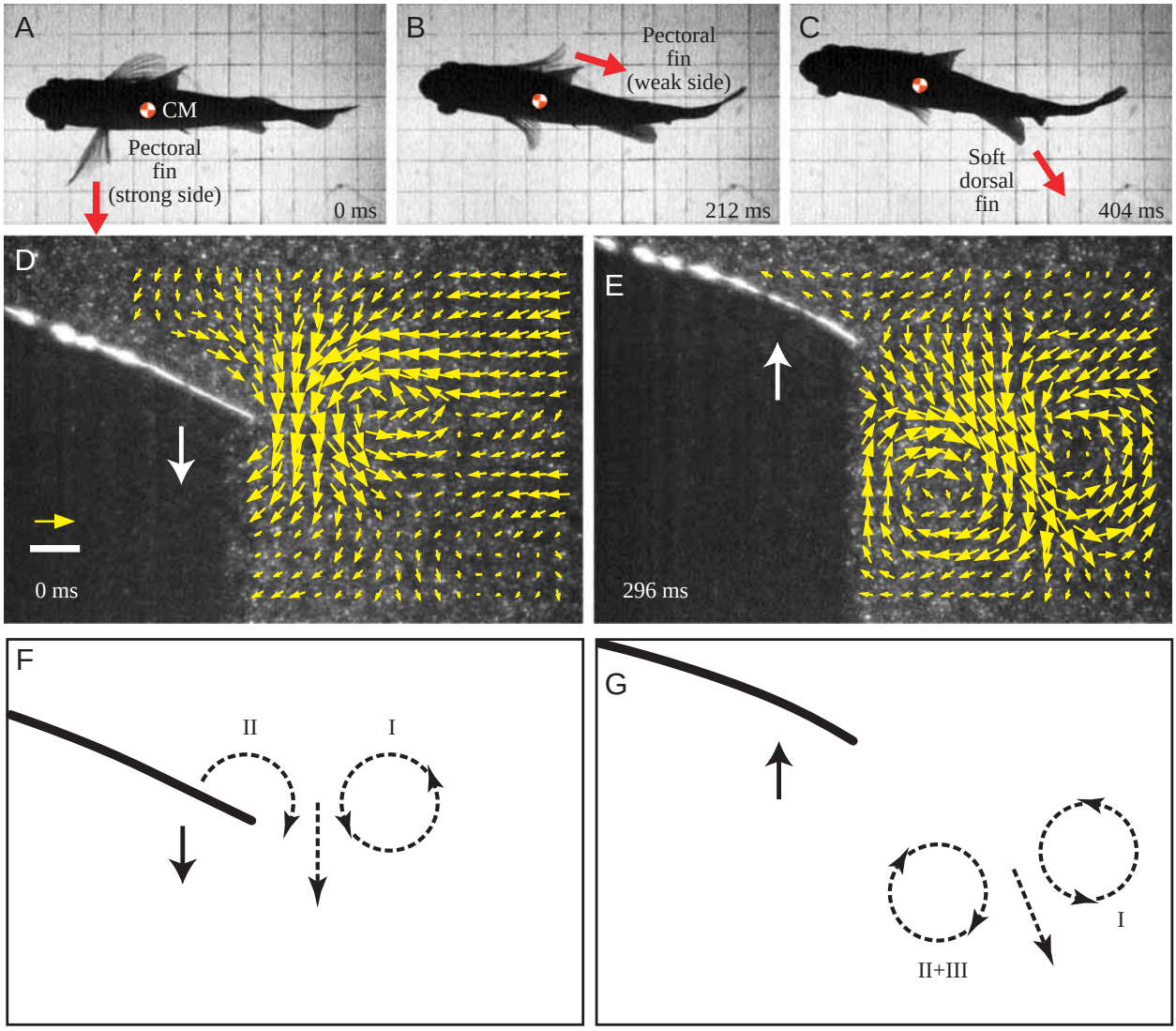

Fig. 5. A low-speed turning maneuver by a sunfish illustrating the propulsive roles of the paired and median fins. In light-video images (A–C), arrows signify the average orientation of jet flow developed by each fin sequentially during the turn. (A) In response to a stimulus issued on the left side of the fish (i.e. at the bottom of the panel), the ipsilateral or 'strong-side' pectoral fin abducts, generating a strong laterally oriented wake flow that rotates the body around the center of mass. (B) The contralateral 'weak-side' pectoral fin subsequently adducts, creating a posteriorly directed fluid jet that initiates forward translation of the body. Details of wake flow produced by the pectoral fins were presented in an earlier study (Drucker and Lauder, 2001). Near the end of the turn (B,C), the soft dorsal fin abducts independently of body bending and generates an obliquely oriented fluid jet. Flow fields in the wake of the soft dorsal fin during turning are presented in D and E for a frontal-plane laser sheet in position 1 (see Fig. 2D). Large solid-line arrows indicate the direction of fin motion. Free-stream velocity of $0.5\,L\,s^{-1}$, where L is total body length, or $10.5\,cm\,s^{-1}$, from left to right has been subtracted from each vector. Schematic representations of observed wake structures are shown in F and G. (D) During abduction of the dorsal fin, a free vortex is shed from the trailing edge (shown as counterclockwise flow), while opposite-sign vorticity develops at the fin tip (cf. Fig. 4B). (E) Upon return of the fin towards the body midline, bound vorticity is shed into the wake to form a second free vortex (cf. Fig. 4C). The momentum of these paired vortices and associated jet flow on the strong side of the body is not balanced by subsequent fin abduction to the opposite side of the body as during steady swimming (Fig. 4). The reaction force acting on the soft dorsal fin posterior to the center of mass of the body serves the dual function of slowing initial pectoral-fin-induced body rotation and helping to propel the animal forward away from the stimulus. CM, center of mass of the body (located at 0.36L posterior to the snout after Webb and Weihs, 1994). Light-video images in A–C are modified from previous work (Drucker and Lauder, 2001). Scales for D and E: arrow, $10\,cm\,s^{-1}$; bar, 1 cm. Vortex labels in F and G are defined in Fig. 4.

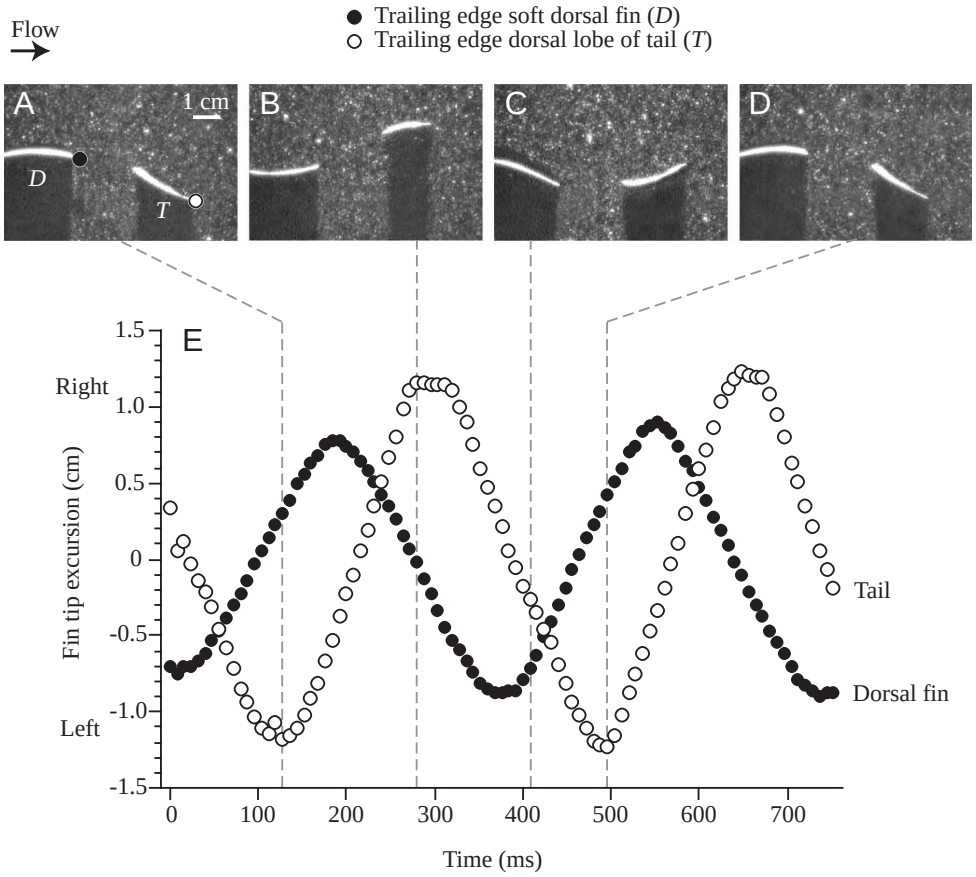

Fig. 6. Kinematic patterns for the soft dorsal fin (*D*) and tail fin (*T*) oscillating in tandem during steady swimming at $1.1\,L\,s^{-1}$, where L is total body length. A–D show video images of the two fins moving within a frontal-plane laser sheet (Fig. 2D, position 2) over the course of one complete stroke cycle. Digitizing such images allowed measurement of temporal and spatial patterns of fin tip excursion. In E, left–right movements of the trailing edges of the soft dorsal fin and the dorsal lobe of the tail are plotted against time for two consecutive stroke cycles. Although both fins oscillate at a frequency of 2.5 Hz, motion of the tail lags behind that of the dorsal fin by an average of 121 ms, or 30 % of the stroke cycle. The abduction amplitude of the tail on each side of the body exceeds that of the dorsal fin by 0.51 cm on average, a difference corresponding to 19 % of the tail's total sweep amplitude.

interaction, and implications for thrust production, are discussed below.

Discussion

Role of the soft dorsal fin in locomotion

This paper provides new information on the motion and hydrodynamic function of the perciform dorsal fin during locomotion and contributes to our understanding of the diversity of propulsive roles played by fish fins in swimming. In a previous study of dorsal-fin locomotor mechanics in *Lepomis macrochirus*, Jayne et al. (Jayne et al., 1996) illustrated occasional abduction of the posterior portion of the dorsal fin during steady swimming, but did not report continuous undulation as observed in this study (e.g. Fig. 4, Fig. 6). Furthermore, non-periodic, unilateral abduction of the soft dorsal fin during turning (Fig. 5) has not previously been documented for perch-like fishes. Below, we examine the relationship between dorsal fin kinematics and hydrodynamic function, specifically addressing the roles played by the soft dorsal fin of sunfish during steady and unsteady swimming.

The pronounced mediolateral excursions of the dorsal fin observed during fast steady swimming (i.e. at speeds involving oscillation of the caudal fin) as well as during unsteady turning

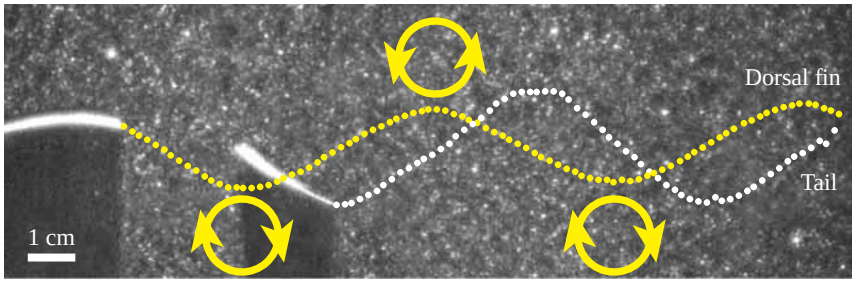

Fig. 7. Sinusoidal paths described by the soft dorsal fin and dorsal lobe of the tail within the horizontal plane (Fig. 2D, position 2) during steady swimming at $1.1\,L\,s^{-1}$, where L is total body length. Flow fields generated separately by each fin are illustrated in Fig. 4 and Fig. 8. Vortices shed by the trailing edge of the soft dorsal fin are represented schematically, but are located in positions determined by analysis of DPIV videos. By virtue of phase-delayed motion and a larger sweep amplitude (Fig. 6), the caudal fin is positioned to intercept wake vortices generated by the dorsal fin.

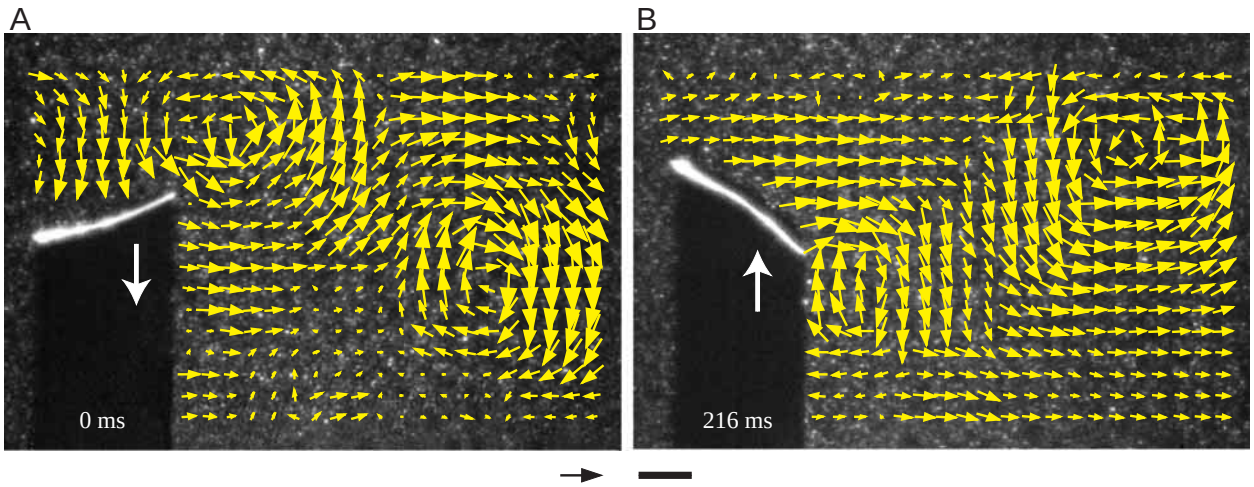

Fig. 8. Representative flow fields in the wake of the oscillating caudal fin of sunfish during steady swimming at 1.1 $L\,s^{-1}$, where L is total body length. Flow patterns within the frontal-plane laser sheet intersecting the tail at mid-fork (Fig. 2D, position 3) are shown for the early stages of two consecutive fin half-strokes. The direction of tail fin motion is indicated by large white arrows. Free-stream velocity (24.7 $cm\,s^{-1}$) from left to right has been subtracted from each velocity vector to reveal vortical wake structures. In general, the wake generated by the tail closely resembles that produced separately by the soft dorsal fin upstream (cf. Fig. 4A,C). Each half-stroke generates vorticity at the trailing edge of the fin that is ultimately released into the wake (counterclockwise flow in A and B). Opposite-sign vorticity attached to the fin (in the upper left-hand corner of A) migrates to the trailing edge over the course of the stroke period (visible at the tip of the fin in B). Repeated cycles of caudal fin oscillation generate a reverse von Kármán vortex street. Scales: arrow, 10 $cm\,s^{-1}$; bar, 1 cm.

raise two functional questions. First, does the dorsal fin move actively and independently from the body to which it is attached? Like the body, whose bending during swimming is powered by contraction of the myotomal musculature, the soft dorsal fin is invested with segmentally arranged muscles capable of controlling mediolateral motion of the propulsive fin surface. On both sides of the body, dorsal inclinator muscles arise from the fascia overlying the epaxial myomeres and insert onto the lateral base of each flexible dorsal fin ray, thereby enabling fin abduction (Arita, 1971; Alexander, 1974; Geerlink and Videler, 1974; Winterbottom, 1974; Jayne et al., 1996). Electromyographic recordings from the dorsal inclinator muscles of bluegill sunfish reveal discrete activity patterns during both steady and unsteady swimming behaviors (Jayne et al., 1996). This result indicates that the soft dorsal fin is not merely a passive vane, but instead has the capacity to serve as an active control surface. During fast steady swimming in sunfish, the onset of dorsal inclinator activity is similar to that of ipsilateral red myomeric muscle at a corresponding longitudinal position. Jayne et al. (Jayne et al., 1996) suggest that such dorsal inclinator activation may serve to stiffen the soft dorsal fin and resist its tendency to bend passively as the body sweeps laterally through the water. The idea that motion of the soft dorsal fin is not completely independent from body bending during steady swimming is supported by two findings of the present study: (i) undulation of the dorsal fin is observed only when axial undulation occurs (cf. Fig. 3, Fig. 4), and (ii) above the gait transition speed, the soft dorsal and caudal fins exhibit nearly identical periods of oscillation (Table 1). However, while the anterior portion of the soft dorsal fin attached to the body should be strongly influenced by axial bending, the free posterior margin (e.g. see Fig. 2A) is capable of independent movement. Light-video motion analyses of the soft dorsal fin and body during steady swimming are still needed to determine the extent to which the traveling waves of bending on the two propulsors are out of phase with each other.

Analysis of unsteady braking maneuvers in *Lepomis macrochirus* (Jayne et al., 1996) reveals a pattern of dorsal inclinator activity that is markedly different from that measured during steady swimming. During deceleration of the body, the dorsal inclinators show activity that overlaps that of myomeres on the contralateral, rather than ipsilateral, side of the animal. This decoupled pattern of activation results in abduction of the caudal and soft dorsal fins in opposite directions – a drag-inducing fin arrangement likened to a ‘sea anchor’ (Breder, 1926, p. 208). The ability of the soft dorsal fin to move actively and independently of the body during maneuvering is also evident during turning behaviors. *L. macrochirus* performs low-speed turns that involve minimal axial bending (Drucker and Lauder, 2001). In the absence of pronounced body undulation, the soft dorsal fin nonetheless exhibits clear abduction (Fig. 5B,C). These empirical results have implications for numerical models used to predict velocity fields in the wake of swimming fish. Biomechanically accurate simulations of fish bodies should ideally include median fins modeled not simply as rigid plates moving in phase with body undulation (e.g. Wolfgang et al., 1999) but as surfaces with free, flexible trailing edges capable of actuation independent from that of the trunk and tail.

A second major question concerning dorsal fin function is whether the soft portion of the fin plays an active role in generating locomotor force. The impact of a harmonically

oscillating body on wake structure and associated fluid force is predicted by the Strouhal number *St* (see equation 1). Experimental studies of a foil in steady forward motion and a combination of heaving and pitching motion (Anderson, 1996; Anderson et al., 1998) reveal that, when $St<0.2$, a loosely organized wake forms that generates very low or negative thrust. In this case, one observes either a 'wavy wake' with no distinct vortex formation or a drag-producing von Kármán street characterized by staggered, counterrotating vortices and a central region of jet flow oriented upstream that reduces the momentum of the incident flow (e.g. Goldstein, 1965, p. 38). As Strouhal number rises to within the range $0.2<St<0.5$, wake structure and force change dramatically: a reverse von Kármán street develops that generates a strong thrust force (see fig. 17 in Anderson et al., 1998). This wake trail consists of paired vortices with opposite-sign rotation and a downstream-directed momentum jet between each vortex pair (von Kármán and Burgers, 1935; Weihs, 1972b; Lighthill, 1975; Triantafyllou et al., 1993; Triantafyllou et al., 2000). For the undulating soft dorsal fin of sunfish swimming at $1.1\,L\,s^{-1}$, *St* averaged 0.19 (Table 1), with most fin beats falling within the range 0.18–0.22, transitional values suggesting the generation of either a drag- or thrust-producing wake. In this study, however, the use of quantitative flow visualization has clearly demonstrated that the dorsal fin plays an active role in generating propulsive force.

During steady swimming above the gait transition speed, frontal-plane flow fields in the wake of the dorsal fin consistently contain a reverse von Kármán street (Fig. 4) whose momentum flow is a source of thrust. Stroke kinematics and patterns of wake flow are remarkably similar for the soft dorsal and caudal fins (cf. Fig. 4, Fig. 8), suggesting that the former functions as a 'second tail' during forward locomotion. Turning maneuvers performed by sunfish, although involving non-periodic dorsal fin movements, also generate fluid flow consistent with thrust production. The pattern shown in Fig. 5F,G, as the dorsal fin completes its abduction and then returns to the body midline, is essentially the portion of a reverse von Kármán street generated by a single stroke of the propulsor during steady swimming (cf. Fig. 4F,G). The soft dorsal fin of sunfish, therefore, generates propulsive force by a similar hydrodynamic mechanism during forward locomotion and turning. For both steady and unsteady swimming behaviors, a key kinematic feature leading to the development of a thrust wake is the rapid stroke reversal at the end of fin abduction. The abrupt change in stroke direction forces vorticity bound to the dorsal fin into the wake (Fig. 4, Fig. 5, vortex II; see also Dickinson and Götz, 1996), which contributes to a central jet flow whose velocity exceeds that of the free-stream flow (Table 1). On the basis of empirical data on wake flow, we conclude that the soft dorsal fin indeed makes an active contribution to the development of propulsive forces during locomotion.

Division of labor among multiple propulsors

Observation of sunfish maneuvering and swimming steadily at high speed reveals the simultaneous, coordinated use of three separate fin systems: the paired pectoral fins, the caudal fin and the soft dorsal fin. At a swimming speed just above the gait transition to combined paired- and median-fin locomotion, the Strouhal number for each active fin falls within the range 0.19–0.31 on average (Table 1; Drucker and Lauder, 1999). Consistent with this finding, each fin generates a propulsive wake (Fig. 4, Fig. 8; see fig. 9 in Drucker and Lauder, 1999). Quantitative wake visualization documents the capacity of these distinct components of the propulsive anatomy to make independent contributions to locomotor force.

Such division of labor among fins can be illustrated by an analysis of unsteady swimming behavior. Previous study of the pectoral fin wake (Drucker and Lauder, 2001) together with new observations of the dorsal fin wake in the present study allow a description of the combined role of paired and median fins in low-speed turning maneuvers. During the initial stage of a slow yawing turn, sunfish abduct the strong-side pectoral fin (i.e. the fin closer to the given stimulus) to generate a strong laterally oriented wake flow (Fig. 5A). The medially directed reaction force on this fin (21 mN on average) is transmitted to the body through the pectoral fin base, which is located approximately 12 % of body length, *L*, anterior to the center of mass of the animal (Drucker and Lauder, 2001); this relative distance corresponds to 2.5 cm on average for the sunfish examined in this study. During DPIV image recording, the fish's center of mass was excluded from the relatively high-magnification field of view, thereby preventing direct measurement of moment arms for turning. In the absence of data on turning moments, however, we propose that the primary role of the strong-side pectoral fin is to exert torque around the center of mass, thereby rotating the body and changing the fish's heading. In the next stage of the turn, the contralateral (weak-side) pectoral fin adducts, generating a large posteriorly directed momentum flow (Fig. 5B) whose reaction (mean 48 mN) helps to translate the body forward (Drucker and Lauder, 2001). In the present study, we observed these early pectoral fin motions to be followed in the latter stages of the turn by activity of the dorsal fin. After the onset of the translational phase of the turn (i.e. upon weak-side pectoral fin adduction), the soft dorsal fin abducts (Fig. 5B,C), playing a previously unrecognized role in unsteady maneuvering propulsion by sunfish. The momentum jet produced by the dorsal fin during turning is at nearly 45 ° to the fish's initial heading, reflecting the generation of lateral and posterior (thrust) forces of comparable magnitude (11 and 13 mN, respectively; Table 1). The medially oriented reaction force exerted on the soft dorsal fin is transmitted to the body posterior to the center of mass (Fig. 5C). Although half that experienced by the strong-side pectoral fin, this inward force acts at a greater distance from the center of mass. For the fish examined in this study, the center of the soft-dorsal fin base is located 21±2 % *L*, or 4.4±0.5 cm (mean ± S.D., $N=4$), posterior to the center of mass (see Webb and Weihs, 1994, in which the center of mass for adult *Lepomis macrochirus* is located at 0.36*L* on average). Accordingly, we predict that an important

locomotor role of the soft dorsal fin is to exert opposite-sign torque at the end of the turn to counter the body rotation generated earlier by the strong-side pectoral fin. In resisting further body rotation, the dorsal fin helps correct the heading of the fish as it begins to translate forward on a linear trajectory away from the stimulus. The relatively large thrust force associated with the dorsal fin during the translational phase of turning (Table 1) suggests that the fin also makes a substantial contribution to this forward propulsion. Low-speed turns in sunfish therefore involve the generation of fluid forces that are both perpendicular and parallel to the longitudinal axis of the body and are applied sequentially by the paired and median fins.

For steady swimming, locomotor force can also be partitioned among multiple active fins. At low speed ($0.5\,L\,s^{-1}$), swimming force is generated solely by the oscillating pectoral fins without contribution from the tail or dorsal fin (Fig. 3; Drucker and Lauder, 1999). At $1.1\,L\,s^{-1}$, in contrast, the median fins of sunfish shed two free vortices into the wake during the kinematic stroke period τ (Fig. 4, Fig. 8). From these paired vortices, stroke-averaged locomotor forces can be calculated for each fin (Table 1). Such values, however, may underestimate the total rate of change in wake momentum over τ. Each complete cycle of median fin oscillation generates two sets of starting and stopping vortices (labeled here and in Fig. 4 in order of appearance I–IV). First, a starting vortex (Fig. 4E, vortex I) is shed as the fully abducted fin begins to move towards the body midline. As the fin decelerates on the opposite side of the body, vorticity bound to the fin develops as a stopping vortex (Fig. 4F, vortex II). However, the rapid stroke reversal that follows results in the fusion of this stopping vortex with the starting vortex (III) of the next half-stroke. A stopping–starting vortex is visible as clockwise flow in Fig. 4G. Finally, as the fin returns to its original abducted position at the end of the stroke, bound vorticity migrates towards the trailing edge of the fin to contribute to a new stopping vortex (Fig. 4H, vortex IV). At the end of the kinematic stroke period, the circulation of such developing vortices (i.e. attached to the fin, but not yet shed into the wake as free centers of vorticity) could not be accurately determined using DPIV analysis. To account for this additional vorticity developed during the stroke period, we used an alternative estimate of force based upon all three contiguous vortex structures formed by each fin stroke (i.e. I, II+III and IV). In Fig. 9, median fin force for steady swimming is reported as twice the mean value calculated for a single pair of free vortices in the wake (as in Table 1). This estimate reflects the production of two linked vortex rings (represented by three frontal-plane vortices) over the course of each complete stroke cycle.

The soft dorsal fin of sunfish is responsible for generating a substantial portion of overall locomotor force. During steady swimming at $1.1\,L\,s^{-1}$, this fin exerts 12 % of the total thrust developed by all three fin systems studied (Fig. 9A). During turning maneuvers, the dorsal fin also serves an important function, producing more than one-third of the total lateral force generated (Fig. 9B). These data provide quantitative support for an active role for the soft dorsal fin in propulsion. Our results highlight the ability of perciform fish to use multiple fins simultaneously and independently for generating locomotor force and for controlling complex swimming behaviors. In addition, there is evidence that this propulsion may be achieved with relatively high efficiency. Studies of man-made foils undergoing heaving and pitching motion (Triantafyllou et al., 1993; Anderson et al., 1998) show that

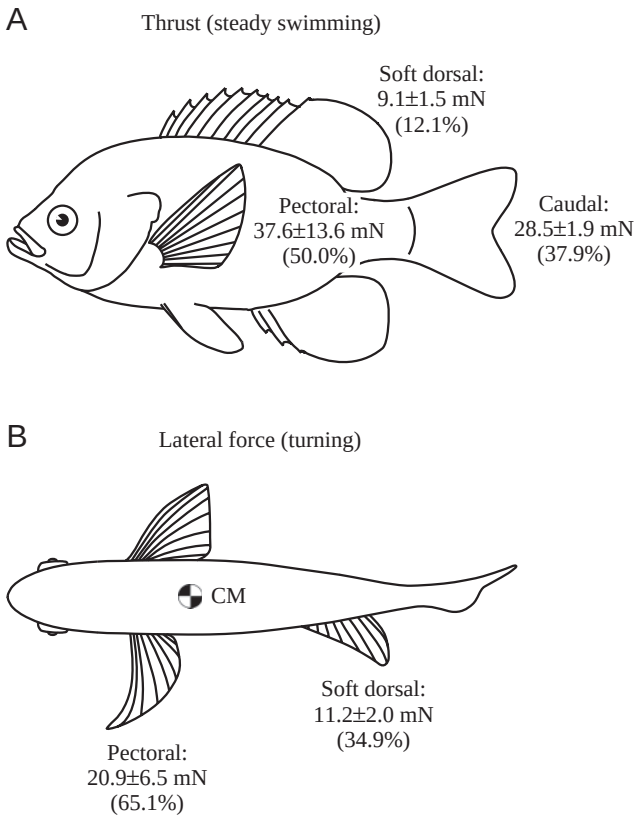

Fig. 9. Summary of stroke-averaged locomotor forces generated by three fin systems in sunfish. Each force is reported as mean ± S.E.M. (N=6–11 fin beats) with the corresponding percentage of total force generated by all fins given in parentheses. (A) Thrust produced during steady swimming at $1.1\,L\,s^{-1}$, where L is total body length. Dorsal and caudal fin forces are calculated from the momentum of three frontal-plane vortices developed during each complete fin stroke period (see Discussion; cf. Table 1). Pectoral fin force is the mean reaction force experienced by both left and right paired fins together over the downstroke–upstroke period (from Drucker and Lauder, 1999). (B) Lateral force generated during turning following steady swimming at $0.5\,L\,s^{-1}$. Since turning involves non-periodic fin motion, mean forces are calculated over the duration of the half-stroke. Pectoral force is for the strong-side fin (from Drucker and Lauder, 2001). The substantial contribution of the soft dorsal fin to locomotor force (12 % thrust and 35 % lateral force) supports an active role for this fin in propulsion. In general, the observed partitioning of force among fins highlights the ability of teleost fishes to use multiple fins simultaneously and independently during locomotion. CM, center of mass of the body (positioned according to Webb and Weihs, 1994).

propulsive efficiency, defined as the ratio of useful power output to total power input, is maximized when Strouhal number falls within the range $0.25<St<0.4$. For *Lepomis macrochirus*, the frequency and amplitude of oscillation of the caudal fin yield Strouhal numbers within this range (Table 1), a result matching that for the tails of many other aquatic vertebrates (Triantafyllou et al., 1993) as well as the pectoral fins of perciform fishes (Walker and Westneat, 1997; Drucker and Lauder, 1999). Further, we find that the soft dorsal fin of steadily swimming sunfish shows an average *St* just below this range of expected peak efficiency (Table 1). Predictions such as these about swimming performance based upon fin kinematics can be tested empirically. In future work, combining study of locomotor muscle performance *in vitro* with quantitative analysis of wake dynamics *in vivo* will allow measurement of the efficiency of transmission of the internal mechanical force developed by the swimming musculature to external fluid force for overcoming drag.

Dorsal–caudal fin wake interaction

The observation that fish can use multiple fins simultaneously to generate separate wake vortices and fluid forces raises the interesting possibility of hydrodynamic interaction among these propulsors. For the specific case of two median fins oscillating in tandem, a modification of elongated-body theory allowing for longitudinal variation in body depth and wake interaction between adjacent fins has been used to predict locomotor force and efficiency (Lighthill, 1970; Wu, 1971b; Yates, 1983; Weihs, 1989). At the trailing edge of the upstream fin, a vortex sheet is shed that carries both momentum and energy downstream. If the downstream fin is of sufficient depth, it will intercept this sheet and reabsorb its vorticity, reducing the loss of wake energy. When the two fins oscillate with a substantial phase difference, the upstream vorticity is hypothesized to augment thrust and the overall propulsive effectiveness (Lighthill, 1970; Wu, 1971a). It should be noted, however, that the concept of the vortex sheet in hydromechanical theory has been used to describe flow in inviscid fluids. For multiple median fins moving in water, an alternative possibility is that each propulsor sheds an array of discrete vortices that may individually coalesce with vortices produced by an adjacent propulsor, thereby influencing wake circulation and force. The nature of such vortex interactions has been explored in greatest depth experimentally in non-biological systems. It has been shown that vortex trails shed by upstream bodies can intercept and affect the strength of developing vortices shed by bodies downstream. For example, the drag wake (von Kármán street) of an upstream bluff body can either strengthen or weaken the circulation of the near-field thrust wake (reverse von Kármán street) produced by a downstream oscillating foil (Gopalkrishnan et al., 1994; Anderson, 1996; Triantafyllou et al., 2000). Whether the interaction is constructive or destructive (i.e. involves a reinforcement or annihilation of vortices) depends on the sign of vortex rotation and the encounter phase of the foil with respect to the upstream wake. For two adjacent hydrofoils shedding a thrust wake, as observed in freely swimming sunfish, the type of vortex interaction is similarly dictated by encounter kinematics.

In the present study, we experimentally examined the hydrodynamic impact of vortices produced by the soft dorsal fin on vortices generated by the tail of *Lepomis macrochirus*. As explained in the Results, particle images in the narrow region between the two fins were contaminated by rapidly changing areas of shadow and bright reflection from the fins themselves (e.g. Fig. 6A–D), which precluded accurate quantification of water velocity fields in this location. Inspection of raw DPIV video, however, revealed consistent patterns of vortex generation by this tandem fin arrangement. As the dorsal fin moves laterally (Fig. 10A,B), it produces a trailing vortex (*a*) that represents a portion of the fin's reverse von Kármán street (cf. Fig. 4E,F, vortex I). This vortex is

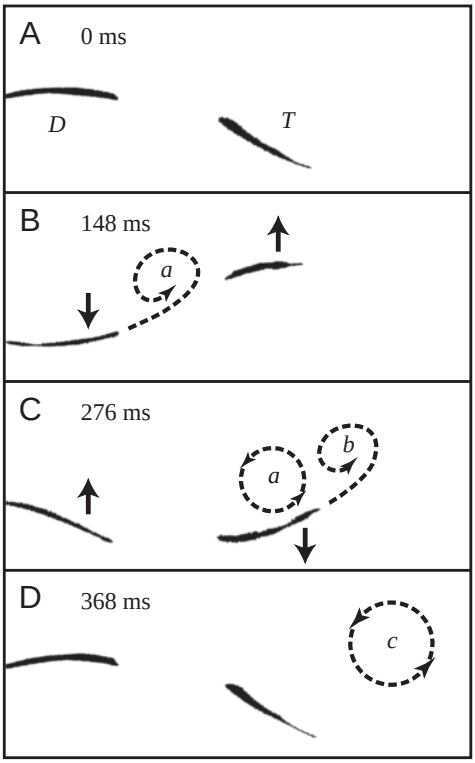

Fig. 10. Constructive wake interaction between the soft dorsal fin (*D*) and the dorsal lobe of the tail (*T*) during steady swimming at $1.1\,L\,s^{-1}$, where *L* is total body length. Silhouettes of the two fins within a frontal-plane laser sheet (Fig. 2D, position 2) are shown moving over the course of one stroke cycle. The direction of fin movement is indicated by solid-line arrows. Vortices observed in the raw DPIV video recording are indicated by dashed lines. Vortex *a* is shed as the soft dorsal fin sweeps laterally (A,B) and migrates downstream during the development of an analogous tail vortex *b* (C). As the tail completes its stroke, the two counterclockwise-rotating vortices coalesce, forming a single larger downstream vortex *c* (D). The process illustrated in A–D is repeated on both sides of the body to yield the tail's reverse von Kármán street wake (cf. Fig. 8). Reinforcement of developing circulation around the tail through interception of the dorsal fin's vortices is proposed as a mechanism for enhancing thrust.

intercepted by the re-entrant dorsal lobe of the tail, which has a larger sweep amplitude than the soft dorsal fin (see Fig. 7). Vortex *a* passes along the surface of the tail while the tail itself develops bound vorticity and finally sheds an analogous vortex (*b*) (Fig. 10C). The two vortices generated by these median fins have the same rotational sense and the correct timing of interaction to merge constructively in the vicinity of the tail, forming a larger, combined vortex *c* (Fig. 10D). We expect the circulation of this combined vortex, although less than the strength of *a* and *b* together, to be greater than the circulation of *a* or *b* alone. It is important to note, however, that, although vortex *c* represents a fusion of two vortices, this structure forms downstream of the tail and therefore does not imply a benefit to force production. We hypothesize that, in the early stage of the tail's half-stroke, the presence of rotational flow from the dorsal fin's wake (vortex *a*) increases incident velocity over the tail and enhances same-sign vorticity bound to the tail (flow that is ultimately shed as vortex *b*; Fig. 10C). Such reinforcement of developing circulation is proposed as a mechanism for adding energy to the tail's wake and for increasing thrust production by the tail.

The phenomenon of wake interaction in freely locomoting animals has been the subject of limited experimental study to date. Wolfgang et al. demonstrated that upstream body-bound vorticity in the teleost fish *Danio malabaricus* can be released downstream to interact constructively with vorticity formed by the oscillating tail (Wolfgang et al., 1999). Flapping insect wings may also benefit from 'wake capture' (Dickinson et al., 1999). In this unsteady mechanism, fluid accelerated during each half-stroke may be exploited by the wing on the return stroke to increase incident velocity and lift. Whether vortex interaction of the type illustrated in Fig. 10 confers any hydrodynamic benefit to bluegill sunfish requires a comparison of the circulation around the tail in the presence and absence of the dorsal fin's wake (cf. Anderson, 1996).

Future directions: interpreting evolutionary variation in dorsal fin design

The evolution of teleost fishes is characterized by an impressive diversification of locomotor anatomy. The dorsal fin, in particular, shows pronounced taxonomic variation in design. The soft-rayed portion of the dorsal fin, for instance, varies widely among species in number, shape and position on the body (Breder, 1926; Harris, 1953; Aleev, 1969; Helfman et al., 1997). Several auxiliary soft fins on the dorsal midline also occur with scattered distribution (e.g. the adipose fin in salmoniform, myctophiform and many ostariophysan fishes and the dorsal finlets in scombroid fishes). In addition, derived acanthopterygian fishes are distinguished from more basal teleosts by the presence of a stiff, spiny dorsal fin positioned anterior to the flexible, soft dorsal fin (Rosen, 1982). Improving our understanding of the functional significance of such evolutionary variation in fin design requires continued experimental study of wake dynamics in freely swimming fishes representing the diverse array of morphologies exhibited by living taxa.

The vortex structures and associated fluid forces measured in this study for the dorsal fin anatomy of sunfish (i.e. fused soft and spiny dorsal fins; see Fig. 1, Perciformes) suggest additional functional hypotheses regarding fin design in other lineages. One such hypothesis concerns the role of the spiny dorsal fin in facilitating the generation of a thrust wake. In *Lepomis macrochirus*, as in other perciform fishes, the spiny dorsal fin is comparatively rigid, with a limited range of mediolateral motion. Between the most posterior fin spine and the most anterior ray of the soft dorsal fin is a robust connective tissue webbing (Jayne et al., 1996). This connection may serve to 'anchor' the soft dorsal fin and provide increased rigidity in its anterior section. Accordingly, we predict that, in plesiomorphic teleosts that lack the spiny dorsal fin (e.g. Clupeiformes, Salmoniformes; see Fig. 1), the soft dorsal fin may be insufficiently stiffened (in spite of activity in the dorsal inclinator muscles) to resist passive bending as the body sweeps laterally through the water. In these fishes, the soft dorsal fin may be a less effective propulsor because of its greater compliance. Using digital particle image velocimetry to study freely swimming salmoniforms, for example, it will be possible to test the prediction that a dorsal fin lacking a spiny section generates a 'wavy' drag wake (Anderson et al., 1998) rather than a thrust-generating reverse von Kármán street.

Flow visualization may also be used to evaluate a number of untested theoretical hypotheses about the functional impact of phylogenetic variation in dorsal fin design. For two or more median fins oscillating in tandem, the significance of the spacing between propulsors has been addressed using hydromechanical theory. When the gap between fins is small (e.g. in gadid fishes and many atheriniforms; see Fig. 1), a vortex sheet is hypothesized to fill the interval, making separate median fins mechanically equivalent to a single, structurally continuous propulsor. Since the surface area of the moving body is reduced between the fins, overall drag is diminished (Lighthill, 1970; Wu, 1971a; Wu, 1971b). Using DPIV, one can visualize whether such vortex sheets in fact develop between fins and test this potentially important mechanism for drag reduction. When the gaps between fins are large (e.g. in basal teleosts, Fig. 1), the theoretical prediction is that thrust can be increased (Lighthill, 1970; Wu, 1971a). The wake interaction of greatest benefit (i.e. resulting in maximal thrust and propulsive efficiency) is hypothesized to occur with an inter-fin distance of $0.4L$ (Weihs, 1989). However, when the median fins are separated by a sufficiently large gap, we predict that overall thrust will be reduced. For plesiomorphic teleosts, our expectation is that the energy of vortices shed by the soft dorsal fin will have dissipated considerably by the time these vortices reach a longitudinal position corresponding to the tail. Accordingly, such fishes are not expected to benefit from the type of wake interaction proposed for sunfish (Fig. 10), in which the two fins are nearly contiguous. Quantitative wake visualization holds considerable promise for illuminating the hydrodynamic significance of evolutionary variation in propulsor morphology.

The authors gratefully acknowledge Erik Anderson, Jamie Anderson, David Beal, John Carling, Michael Dickinson, Paul Webb, Danny Weihs and Thelma Williams for helpful discussions and commentary on the ideas presented in this paper. Supported by NSF grants DBI-9750321 to E.G.D., IBN-9807012 to G.V.L. and IBN-0090896 to E.G.D. and G.V.L.

References

Aleev, Y. G. (1969). *Function and Gross Morphology in Fish* (translated from the Russian by M. Raveh). Jerusalem: Keter Press.

Alexander, R. McN. (1974). *Functional Design in Fishes*, third edition. London: Hutchinson & Co.

Anderson, J. (1996). Vorticity control for efficient propulsion. PhD thesis, MIT/WHOI, 96-02.

Anderson, J. M., Streitlien, K., Barrett, D. S. and Triantafyllou, M. S. (1998). Oscillating foils of high propulsive efficiency. *J. Fluid Mech.* **360**, 41–72.

Arita, G. S. (1971). A re-examination of the functional morphology of the soft-rays in teleosts. *Copeia* **1971**, 691–697.

Arreola, V. I. and Westneat, M. W. (1996). Mechanics of propulsion by multiple fins: kinematics of aquatic locomotion in the burrfish (*Chilomycterus schoepfi*). *Proc. R. Soc. Lond. B* **263**, 1689–1696.

Blake, R. W. (1976). On seahorse locomotion. *J. Mar. Biol. Ass. U.K.* **56**, 939–949.

Blake, R. W. (1977). On ostraciiform locomotion. *J. Mar. Biol. Ass. U.K.* **57**, 1047–1055.

Blake, R. W. (1978). On balistiform locomotion. *J. Mar. Biol. Ass. U.K.* **58**, 73–80.

Braun, J. and Reif, W. (1985). A survey of aquatic locomotion in fishes and tetrapods. *N. Jb. Geol. Paläont. Abh.* **169**, 307–332.

Breder, C. M., Jr (1926). The locomotion of fishes. *Zoologica* **4**, 159–296.

Breder, C. M., Jr and Edgerton, H. E. (1942). An analysis of the locomotion of the seahorse, *Hippocampus*, by means of high speed cinematography. *Ann. N.Y. Acad. Sci.* **43**, 145–172.

Brodsky, A. K. (1991). Vortex formation in the tethered flight of the peacock butterfly *Inachis io* L. (Lepidoptera, Nymphalidae) and some aspects of insect flight evolution. *J. Exp. Biol.* **161**, 77–95.

Brodsky, A. K. (1994). *The Evolution of Insect Flight.* Oxford: Oxford University Press.

Dickinson, M. H. (1996). Unsteady mechanisms of force generation in aquatic and aerial locomotion. *Am. Zool.* **36**, 537–554.

Dickinson, M. H. and Götz, K. G. (1996). The wake dynamics and flight forces of the fruit fly *Drosophila melanogaster*. *J. Exp. Biol.* **199**, 2085–2104.

Dickinson, M. H., Lehmann, F. O. and Sane, S. P. (1999). Wing rotation and the aerodynamic basis of insect flight. *Science* **284**, 1954–1960.

Drucker, E. G. and Lauder, G. V. (1999). Locomotor forces on a swimming fish: three-dimensional vortex wake dynamics quantified using digital particle image velocimetry. *J. Exp. Biol.* **202**, 2393–2412.

Drucker, E. G. and Lauder, G. V. (2000). A hydrodynamic analysis of fish swimming speed: wake structure and locomotor force in slow and fast labriform swimmers. *J. Exp. Biol.* **203**, 2379–2393.

Drucker, E. G. and Lauder, G. V. (2001). Wake dynamics and fluid forces of turning maneuvers in sunfish. *J. Exp. Biol.* **204**, 431–442.

Fricke, H. and Hissmann, K. (1992). Locomotion, fin coordination and body form of the living coelacanth *Latimeria chalumnae*. *Env. Biol. Fish.* **34**, 329–356.

Geerlink, P. J. and Videler, J. J. (1974). Joints and muscles of the dorsal fin of *Tilapia nilotica* L. (Fam. Cichlidae). *Neth. J. Zool.* **24**, 279–290.

Goldstein, S. (1965). (ed.) *Modern Developments in Fluid Dynamics*, vol. 1. New York: Dover.

Gopalkrishnan, R., Triantafyllou, M. S., Triantafyllou, G. S. and Barrett, D. (1994). Active vorticity control in a shear flow using a flapping foil. *J. Fluid Mech.* **274**, 1–21.

Gordon, M. S., Hove, J. R., Webb, P. W. and Weihs, D. (2000). Boxfishes as unusually well-controlled autonomous underwater vehicles. *Physiol. Biochem. Zool.* **73**, 663–671.

Gosline, W. A. (1971). *Functional Morphology and Classification of Teleostean Fishes*. Honolulu: University of Hawaii Press.

Grodnitsky, D. L. and Morozov, P. P. (1992). Flow visualization experiments on tethered flying green lacewings *Chrysopa dasyptera*. *J. Exp. Biol.* **169**, 143–163.

Grodnitsky, D. L. and Morozov, P. P. (1993). Vortex formation during tethered flight of functionally and morphologically two-winged insects, including evolutionary considerations on insect flight. *J. Exp. Biol.* **182**, 11–40.

Harris, J. E. (1936). The role of the fins in the equilibrium of the swimming fish. I. Wind tunnel tests on a model of *Mustelus canis* (Mitchell). *J. Exp. Biol.* **13**, 476–493.

Harris, J. E. (1937). The mechanical significance of the position and movements of the paired fins in the Teleostei. *Pap. Tortugas Lab.* **31**, 173–189.

Harris, J. E. (1953). Fin patterns and mode of life in fishes. In *Essays in Marine Biology* (ed. S. M. Marshall and A. P. Orr), pp. 17–28. Edinburgh: Oliver & Boyd.

Helfman, G. S., Collette, B. B. and Facey, D. E. (1997). *The Diversity of Fishes*. Malden, MA: Blackwell Science.

Jayne, B. C., Lozada, A. F. and Lauder, G. V. (1996). Function of the dorsal fin in bluegill sunfish: motor patterns during four distinct locomotor behaviors. *J. Morph.* **228**, 307–326.

Lauder, G. V. (2000). Function of the caudal fin during locomotion in fishes: kinematics, flow visualization, and evolutionary patterns. *Am. Zool.* **40**, 101–122.

Lauder, G. V. and Liem, K. F. (1983). The evolution and interrelationships of the actinopterygian fishes. *Bull. Mus. Comp. Zool.* **150**, 95–197.

Liao, J. and Lauder, G. V. (2000). Function of the heterocercal tail in white sturgeon: flow visualization during steady swimming and vertical maneuvering. *J. Exp. Biol.* **203**, 3585–3594.

Lighthill, M. J. (1969). Hydromechanics of aquatic animal propulsion: a survey. *Annu. Rev. Fluid Mech.* **1**, 413–446.

Lighthill, M. J. (1970). Aquatic animal propulsion of high hydromechanical efficiency. *J. Fluid Mech.* **44**, 265–301.

Lighthill, M. J. (1975). *Mathematical Biofluiddynamics*. Philadelphia: Society for Industrial and Applied Mathematics.

Lighthill, J. and Blake, R. (1990). Biofluiddynamics of balistiform and gymnotiform locomotion. Part 1. Biological background, and analysis by elongated-body theory. *J. Fluid Mech.* **212**, 183–207.

Lindsey, C. C. (1978). Form, function, and locomotory habits in fish. In *Fish Physiology*, vol. VII (ed. W. S. Hoar and D. J. Randall), pp. 1–100. New York: Academic Press.

Milne-Thomson, L. M. (1966). *Theoretical Aerodynamics*, fourth edition. New York: Macmillan.

Nelson, J. S. (1994). *Fishes of the World*, third edition. New York: John Wiley & Sons.

Raffel, M., Willert, C. E. and Kompenhans, J. (1998). *Particle Image Velocimetry: A Practical Guide*. Heidelberg: Springer-Verlag.

Rosen, D. E. (1982). Teleostean interrelationships, morphological function and evolutionary inference. *Am. Zool.* **22**, 261–273.

Spedding, G. R., Rayner, J. M. V. and Pennycuick, C. J. (1984). Momentum and energy in the wake of a pigeon (*Columba livia*) in slow flight. *J. Exp. Biol.* **111**, 81–102.

Triantafyllou, G. S., Triantafyllou, M. S. and Grosenbaugh, M. A. (1993). Optimal thrust development in oscillating foils with application to fish propulsion. *J. Fluids Struct.* **7**, 205–224.

Triantafyllou, M. S., Triantafyllou, G. S. and Yue, D. K. P. (2000). Hydrodynamics of fishlike swimming. *Annu. Rev. Fluid Mech.* **32**, 33–53.

von Kármán, T. and Burgers, J. M. (1935). General aerodynamic theory. Perfect fluids. In *Aerodynamic Theory*, vol. II (ed. W. F. Durand), p. 308. Berlin: Springer-Verlag.

Walker, J. A. and Westneat, M. W. (1997). Labriform propulsion in fishes: kinematics of flapping aquatic flight in the bird wrasse *Gomphosus varius* (Labridae). *J. Exp. Biol.* **200**, 1549–1569.

Webb, P. W. (1977). Effects of median-fin amputation on fast-start performance of rainbow trout (*Salmo gairdneri*). *J. Exp. Biol.* **68**, 123–135.

Webb, P. W. (1993). Swimming. In *The Physiology of Fishes, CRC Marine Science Series* (ed. D. H. Evans), pp. 47–73. Boca Raton, FL: CRC Press.

Webb, P. W. and Keyes, R. S. (1981). Division of labor between median fins in swimming dolphin fish. *Copeia* **1981**, 901–904.

Webb, P. W. and Weihs, D. (1994). Hydrostatic stability of fish with swim bladders: not all fish are unstable. *Can. J. Zool.* **72**, 1149–1154.

Weihs, D. (1972a). A hydrodynamic analysis of fish turning manoeuvres. *Proc. R. Soc. Lond. B* **182**, 59–72.

Weihs, D. (1972b). Semi-infinite vortex trails, and their relation to oscillating airfoils. *J. Fluid Mech.* **54**, 679–690.

Weihs, D. (1973). The mechanism of rapid starting of slender fish. *Biorheology* **10**, 343–350.

Weihs, D. (1989). Design features and mechanics of axial locomotion in fish. *Am. Zool.* **29**, 151–160.

Willert, C. E. and Gharib, M. (1991). Digital particle image velocimetry. *Exp. Fluids* **10**, 181–193.

Winterbottom, R. (1974). A descriptive synonymy of the striated muscles of the Teleostei. *Proc. Acad. Nat. Sci. Philadelphia* **125**, 225–317.

Wolfgang, M. J., Anderson, J. M., Grosenbaugh, M., Yue, D. and Triantafyllou, M. (1999). Near-body flow dynamics in swimming fish. *J. Exp. Biol.* **202**, 2303–2327.

Wu, T. Y. (1971a). Hydromechanics of swimming fishes and cetaceans. *Adv. Appl. Mech.* **11**, 1–63.

Wu, T. Y. (1971b). Hydromechanics of swimming propulsion. Part 3. Swimming and optimum movements of slender fish with side fins. *J. Fluid Mech.* **46**, 545–568.

Yates, G. T. (1983). Hydromechanics of body and caudal fin propulsion. In *Fish Biomechanics* (ed. P. W. Webb and D. Weihs), pp. 177–213. New York: Praeger.